

Optoacoustic tomography in preclinical research: *in vivo* distribution of highly purified PEG-coated gold nanorods

Richard Su^{1,2}, Anton Liopo¹, Sergey A. Ermilov¹, Hans-Peter Brecht¹,
Kirill Larin² and Alexander A. Oraevsky^{1,2}

1. TomoWave Laboratories Inc. 675 Bering Dr., Suite 575, Houston, TX 77057

2. Biomedical Engineering Department, University of Houston, Houston, Texas 77004

ABSTRACT

We report on the optoacoustic (OA) imaging of the whole mouse body using a biocompatible contrast agent – highly purified, pegylated gold nanorods (GNR) – which has strong optical absorption in the near-infrared region and low level of toxicity. In vitro toxicity studies showed no significant change in survival rates of the cultured normal epithelium IEC-6 cells when incubated for 24 hours with up to 1 nM of GNR. In vivo toxicity studies in nude mice showed no pathological changes in liver 1 month after the IV injection of GNR with intra-body concentration around 0.25-0.50 nM. In order to study the enhancement of the OA contrast and accumulation of GNR in different tissues, we performed 3D OA imaging of live nude mice with IV-injected GNR. The enhancement of the OA contrast in comparison with the images of the untreated mice was visible starting 1 hour after the GNR injection. The OA contrast of kidneys, liver, and spleen peaked at about 2-3 days after the administration of the GNR, and then was gradually reducing.

Keywords: PEG-coated gold nanorods, toxicity, biodistribution kinetics, 3D tomography.

Correspondence author: Richard Su, email rs@tomowave.com; www.tomowave.com

1. INTRODUCTION

Three-dimensional optoacoustic (OA) tomography has been successfully used to visualize the blood circulation system and certain blood-rich organs, like kidneys and spleen within live mice [1-3]. In those studies, the high-contrast of OA imaging was provided by strong optical absorption of the native hemoglobin [1]. However, in order to be able to see other biological tissues, including malignant tumors, tissue-specific enhancement of optical absorption contrast must be developed. One proposed method is to inject biocompatible gold nanorods (GNR), which have extremely high optical absorption in the near infrared region [4, 5], into the animal's bloodstream. Following the injection, GNR should distribute inside the body according to their modified affinity, therefore, enhancing the optical contrast of the targeted tissues. GNR have been discussed not only as a manner of increasing optical contrast in certain areas, but also as an instrument for localized photothermal therapy. [2, 4] In these studies, we adopted the published methodology of GNR fabrication [2, 6-9] to get a high yield of narrow band GNR with the optical absorption band centered at 760 nm. The manufactured nanorods were pegylated to become non-toxic in animals, and were injected intravenously in the mice's tails as biocompatible OA contrast agents. Eventually, we analyzed the biodistribution of non-functionalized GNR in vivo, using three-dimensional OA images.

2. MATERIAL AND METHODS

2.1 Fabrication, purification and pegylation of gold nanorods

In a typical procedure [10-12], 0.250 mL of an aqueous 0.01 M solution of $\text{HAuCl}_4 \cdot 3\text{H}_2\text{O}$ was added to 7.5 mL of a 0.1 M CTAB solution in a test tube. Then, 0.600 mL of an aqueous 0.01 M ice-cold NaBH_4 solution was added all at once. After 2 hours 18 μL of this seed solution was added to 10 mL of growth solution containing 9.44 mL of 0.10 M CTAB, 0.40

mL of 0.01 M $\text{HAuCl}_4 \cdot 3\text{H}_2\text{O}$, and different volume (from 0.02 to 0.40 mL) of 0.01 M AgNO_3 solutions and add in that order, one by one. Then 0.032 mL of 0.10 M Ascorbic Acid was added. [10] After that the solution was left under thermostatic conditions for 24 hours at the temperature of 30° C. GNR with high aspect ratio and plasmon resonance more then 850 nm was fabricated with binary surfactant mixture of benzyldimethylhexadecylammoniumchloride (BDAC) and CTAB [9]. GNR of different aspect ratio was prepared and presented on figure 1.

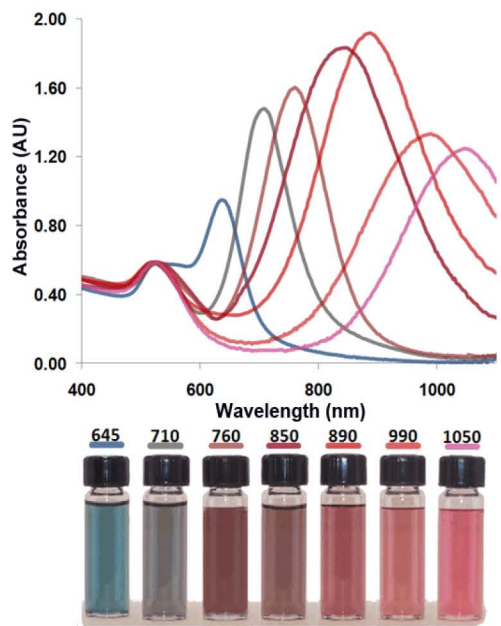


Fig.1 Near-infrared absorption spectra of GNR with gradually increasing aspect ratio

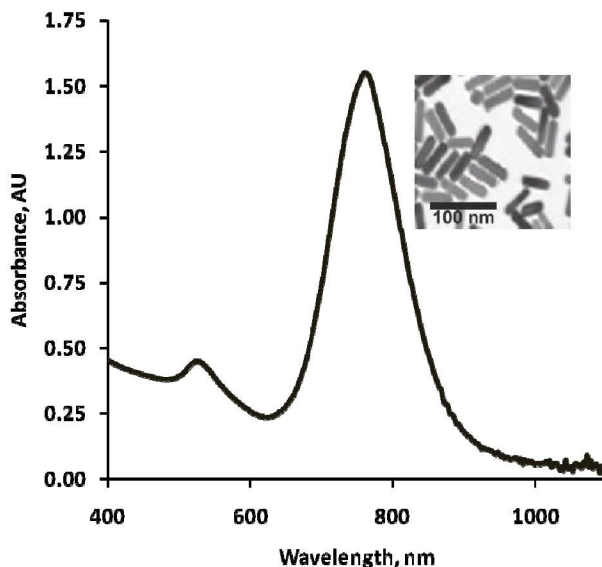


Fig.2 Absorption spectra of GNR with maximum plasmon resonance around 760 nm used in this study

From these different solutions we produced in this study only GNR with maximum absorption around 760 nm. Before covalent binding with Poly(ethylene-glycol), (PEG), the GNR were centrifuged at low speed (4000 rpm, 20 min) for

separation of other aggregates (platelets, stars). The pellet was removed and for the next steps, only the supernatant fraction was used. For conjugation with PEG [12] the solution of GNR was centrifuged at 14,000 g for 10 minutes, the supernatant was removed, and the pellet was resuspended in DI water to reduce CTAB concentration. Then, 0.1 ml of 2 mM potassium carbonate (K_2CO_3) was added to 1 ml of aqueous GNR solution and 0.1 ml of 0.1 mM mPEG-Thiol-5000 (Laysan Bio Inc., Arab, AL). The resulting mixture was kept on a rocking platform at room temperature overnight. Excess mPEG thiol was removed from solution by two rounds of centrifugation and final resuspension in PBS (pH 7.4). The GNR-PEG conjugate was filtered through a 0.22 μ m Millipore Express Plus Membrane which it is important to note that the filtration does not change the properties of GNR. An increase in concentration of pegylated GNR was made by centrifugation at 12,000 g for 10 minutes with the supernatant being removed and the pellet resuspended in PBS pH 7.4 up to a concentration of 12.5 nM (or an optical density around 50, measured from a Thermo Scientific Evolution 201 Spectrophotometer). High purified GNR UV VIS spectra can be seen in Figure 2.

2.2 Cell culture

Normal epithelium IEC-6 cell line was obtained from the American Type Culture Collection (ATTC number CRL 1592) and cultured in DMEM medium with 4 mM L-glutamine adjusted to contain 1.5 g/L sodium bicarbonate and 4.5 g/L glucose and supplemented with 0.1 Unit/ml bovine insulin, 10% fetal bovine serum, 100 U/ml penicillin, and 100 mg/ml streptomycin at 37°C in a humidified atmosphere of 5% CO_2 and 95% air. To examine cell survival from dose dependent effects of PEG-GNR, we seeded IEC-6 cells at a density of 10^5 cells/ml in 0.5 ml of media. The media was changed 3 h after before GNR application in concentration from 0.125 to 5 nM on 24 hours. After this, cells were resuspended (using trypsin and PBS), and stained with Trypan blue in order to count the number of dead and living cells.

All experimental data (each point is 4 measures) presented is analyzed as mean \pm SD

2.3 Optoacoustic imaging of mice

We used commercial prototype of a three-dimensional optoacoustic tomography system developed for preclinical research at TomoWave Labs. The imaging module utilized a water tank with accurate temperature control. The detection system utilized a custom made arc-shaped array of 64 piezo-composite elements with a radius of 65mm. The elements served as ultrawide-band ultrasonic transducers with a center frequency of 3.1 MHz (Imasonic SAS, France). An Nd:YAG pumped Ti: Sapphire laser with 8 ns pulse duration and 10 Hz repetition rate (SpectraWave model, customized for the preclinical imaging system by Quanta Systems (Italy) tuned at 765nm, was attached to a randomized fiber bundle that had four rectangular outputs aligned in orthogonal and backward mode in respect to the transducer array which were located on the outside of an octagonal water tank as described in detail our previous articles [1-3]. Setup of the mouse scanning system with rectangular fiber bundles present on figure 3.



Fig. 3 – Setup of the mouse scanning system with rectangular fiber bundles.

Athymic Nude-Foxn1^{nu} mice (Harlan, Indianapolis, Indiana) were chosen to be the mice scanned. Age and weight of the animals were 7-9 weeks and 23-27 g, respectively. The mice were given isoflurane at 3% as an anesthesia agent. The mice were first scanned prior to any sort of injection to act as a control or baseline to compare. The same mouse was taken out and given a shot of the GNR-PEG, which is described above, intravenously through the tail vein. Optoacoustic scans were done an hour after IV injection and periodically 8 days after. The mice were sacrificed at 24, 72 and 192 h after the IV injections of GNR, with the livers being extracted for liver slices that were prepared and stained with Hematoxylin and Eosin according to the manufacturer's instruction. The GNR injections were of a volume of 400 μ L in sterile PBS with concentration 7.5×10^{12} GNR/mL or 12.5 nM. It is equivalent to 0.25 – 0.50 nM after taking in consideration of the mouse body diluting around 50-70 time (dependence from weight of mouse). Signal processing included deconvolved signals to account for the system transfer function and filtering up to seven scales of wavelets. [3] Reconstruction was done by a custom designed 3D algorithm utilizing the filtered radial back projection after the application of the signal deconvolution and integrated wavelets. Due to the arc shape and object rotation, there is a higher density of transducers at the poles of the sphere of transducers but are weighted accordingly to ensure equal contributions of signal samples to each voxel of the reconstruction globe [3]. Image processing was held constant in all images of the mice so as to be able to compare qualitatively each image. This means that all image brightness, grey scale, gradients, to the image filter being a 3 voxel median filter remained the same so as to be able to compare by qualitative means.

3. Results and Discussion

The quality of pegylating GNR was investigated in vitro. The plasmon band position on the gold nanorods makes it possible to use GNR which absorb in the biological “water window” [5,10,13-15]. Pegylated GNR stability lasts several months and corresponds with data from different groups [3,13-15]. IEC-6 cells were incubated with different PEG-GNR solutions up to 24 hours (fig.4). Cells survived until a GNR concentration of 2 nM as it corresponds with several literature data. [14,16-18] After PEG-GNR injection, Hematoxylin and Eosin Stain of mouse liver following did not show any pathological effects during month (fig. 5) and the data is similar with publications. [4,18-20].

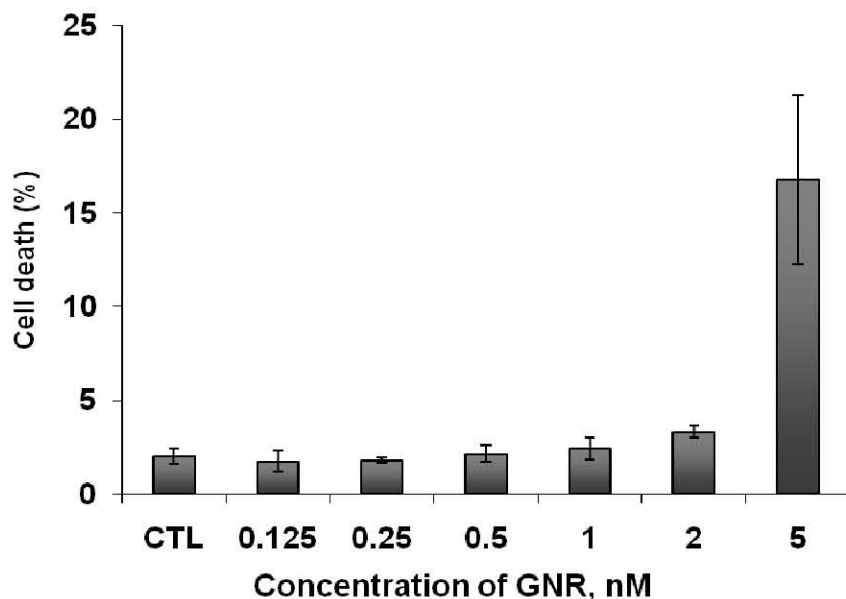


Fig.4 Dose dependence effects of Pegylated GNR on survival of IEC-6 cells (24 hours incubation)

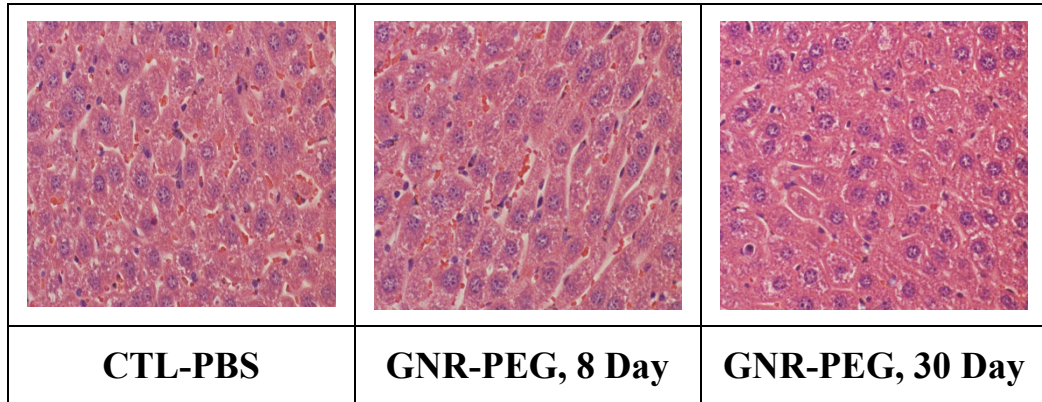


Fig.5 Hematoxylin and Eosin stain of Pegylated GNR (GNR-PEG) accumulating in mouse liver following intravenous (IV) injection

Figure 6 are three-dimensional OA reconstructions from the scans taken from the rotational tomography system with a voxel resolution of 0.1mm. We used a commercial 3D image visualization package from Kitware (VolView-2.0) along with the inherent image processing techniques provided within the software. The Scalar Opacity Mapping allowed us to zero out regions of noise below a designated image brightness of -0.5 which then increased linearly onward to opacity of 0.5 to an image brightness of 3. Finally from the image brightness of 3, it would linearly increase to the full opacity of 1 at the maximum image brightness. This creates a transparency effect based on image voxel brightness where noise would be more or less transparent to emphasize brighter regions. Under the Scalar Color Mapping, a color value of 0 (black) was placed at -3 image brightness that would change to white at an image brightness of 6 and remain white from thereon afterwards. A grey scale color map is created in this case where white is of interest. The Gradient Opacity Mapping set the gradients below 0.22 to be zeroed and then linearly increased to opacity of 1 at a gradient of 1.1 and remains there onwards. This is a second opacity multiplier that deals with the second derivative to emphasize borders. Finally a 3 voxel median filter was applied to all images to help smooth out and decrease remaining noise.

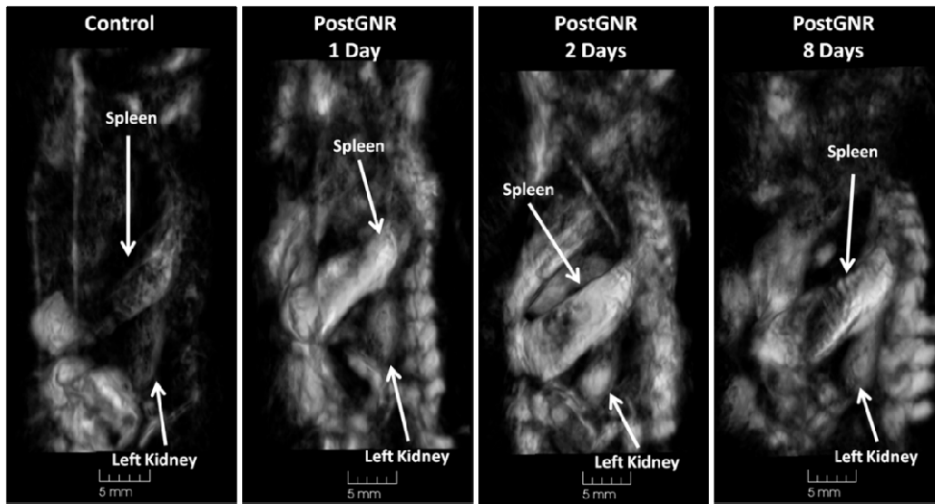


Fig.6 Optoacoustic images of left side of nude mice after IV injection PEG-GNR solution

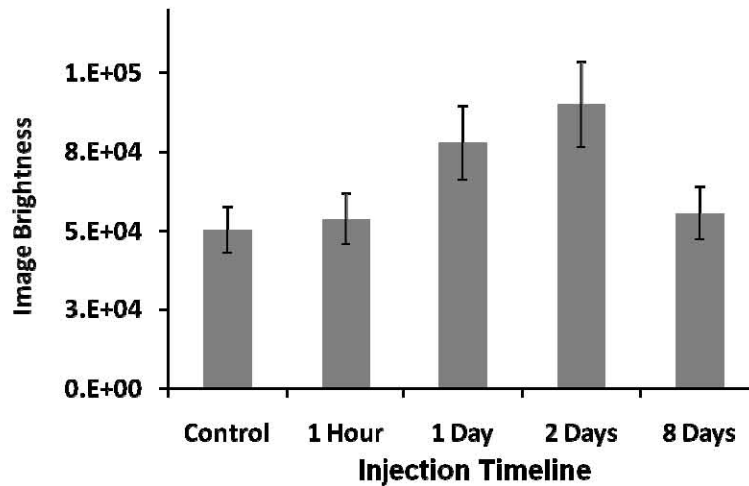


Fig.7 Dynamic brightness of Optoacoustic images of nude mice after IV injection PEG-GNR solution (area of left kidney)

In terms of voxel brightness, if the prior to GNR injection were taken as the base/control then after an hour there is a slight increase followed by a more significant increase in brightness after 24 hours which almost doubles after 48 h and finally decreases 8 days later. This is seen in figure 7 within the left kidney. The dynamic of brightness in OA images in mice after IV injection PEG-GNR solution demonstrated a similar trend with maximum of signal 2 days after injection. We know that strong light extinction (absorption and scattering) of gold nanorods has been employed in various biomedical imaging applications [14,17,21,22]. We investigated with H&E staining which showed no visible differences between the PBS control and the GNR slices. As we know the hepatotoxicity (liver damage) occurs because of the accumulation of nanomaterials in the liver (and spleen) are being taken up by the reticuloendothelial system (part of the immune system where complex components communicate to identify, capture, and filter foreign antigens and particulates) which could lead to hepatotoxicity [17,21]. Looking at H&E stain of liver (Fig.5) we did not find any significant morphological damage of any consequence after GNR administration until 1 month in the liver of mice. The toxicity of the fabricated PEG-GNR which was injected intravenously in the mice is determined to be minimal. We used 20 mg/kg body mass PEG-GNR, but was published [21] data studied the toxicity of PEG modified gold nanoparticles (around 4 g/kg) in mice and found that the nanoparticles accumulate in the liver 168 h after injection, and can induce acute inflammation and cellular damage in the mouse liver and it was not found significant physiological changes in tissues and serum after GNR IV injection until two weeks [4]. This is a strong indication that our purified and pegylated GNR conjugates are not toxic for mice in our dosages which showed improved optoacoustic contrast within images.

4. CONCLUSION

Pegylated GNR distributes themselves within the circulatory system of mice within an hour or two, while still not accumulating in any specific organs. After two days, we observed a maximum increase of GNR within certain organs, such as the kidneys, spleen, and liver. Excised liver tissue, which underwent silver staining, showed maximum GNR concentrations achieved at 2-3 days after their IV administration. The fabricated PEG-modified GNR were determined to be minimally toxic or completely nontoxic for rodents. It was demonstrated that there were significant changes in brightness of reconstructed OA images caused by accumulation of GNR, which implies that OA imaging can be used to track the distribution of untargeted and targeted GNR in vivo.

Acknowledgments

This work was supported in part by an SBIR grant R44CA117986 from the National Cancer Institute. Authors are thankful to M. Phillip Zamora for editing and technical support in preparation of this article.

5. REFERENCES

1. Brecht HP, Su R, Fronheiser M., Ermilov S. A., Conjusteau A., Oraevsky A. A., "Whole Body Three-Dimensional Optoacoustic Tomography System for Small Animals," J. Biomed. Opt. 14, 064007 (2009).
2. R. Su, H.-P. Brecht, S. A. Ermilov, V. Nadvoretzky, A. Conjusteau, A. A. Oraevsky, "Towards Functional Imaging using the optoacoustic 3D whole-body tomography system", Proc. of SPIE 7564, (2010).
3. Su R., Liopo A.V., Brecht H., Ermilov S.A., Oraevsky, A.A. Gold nanorod distribution in mouse tissues after intravenous injection monitored with optoacoustic tomography. *Photons Plus Ultrasound: Imaging and Sensing 2011*, Ed. by Alexander A. Oraevsky A.A., Wang L.W., Proceedings of SPIE Vol. 7899, 78994B. (2011)
4. Kopwiththaya A., Yong K-T, Hu R., Roy I., Ding H., Vathy L.A., Bergey E.J., Paras N Prasad P.N. Biocompatible PEGylated gold nanorods as colored contrast agents for targeted *in vivo* cancer applications *Nanotechnology* **21** (2010) 315101 (10pp)
5. Oraevsky, A. A. Gold and silver nanoparticles as contrast agents for optoacoustic imaging. In *Photoacoustic imaging and spectroscopy*, 1st ed.; Wang, L., Ed.; Taylor and Francis Group: New York; Chapter 30 (2008).
6. Eghtedari M, Oraevsky AA, Copland JA, Kotov NA, Conjusteau A, Motamedi M. High sensitivity of *in vivo* detection of gold nanorods using a laser optoacoustic imaging system. *Nano letters*. 2007;7(7):1914-8.
7. Eghtedari M, Liopo AV, Copland JA, Oraevsky AA, Motamedi M. Engineering of Hetero-Functional Gold Nanorods for the *in vivo* Molecular Targeting of Breast Cancer Cells. *Nano letters*. 2009;9(1):287-91.
8. Niidome, T., Yamagata, M., Okamoto, Y., Akiyama, Y., Takahashi, H. and Kawano, T., "PEG-modified gold nanorods with a stealth character for *in vivo* applications," *Journal of Controlled Release* 114(3), 343-347 (2006).
9. Nikoobakht B., El-Sayed M.A. Preparation and Growth Mechanism of Gold Nanorods (NRs) Using Seed-Mediated Growth Method. *Chem. Mater*. 2003, *15*, 1957-1962
10. Liao H., Hafner J., Gold Nanorod Bioconjugates. *Chem. Mater*. 2005; 17:4636-4641.
11. Huang XH, El Sayed IH, Qian W, El Sayed MA. Cancer cell imaging and photothermal therapy in the near-infrared region by using gold nanorods. *Journal of the American Chemical Society* 2006;128(6):2115-20.
12. Liopo A., Conjusteau A., Konopleva M., Andreeff M., Oraevsky A. Photothermal therapy of acute leukemia cells in the near-infrared region using gold nanorods CD-33 conjugates. *Optical Interactions with Tissue and Cells XXII*. Ed. By Jansen E.D., Thomas R.J., Proceedings of SPIE Vol. 7897, 789710. (2011)
13. Dobrovolskaia MA, McNeil SE Immunological properties of engineered nanomaterials. *Nat Nanotechnol* 2:469–478 (2007).
14. Stone JW, Sisco PN, Goldsmith EC, Baxter SC, Murphy CJ Using gold nanorods to probe cell-induced collagen deformation. *Nano Lett* 7:116–119
15. Alkilany A. M., Murphy C. J. Toxicity and cellular uptake of gold nanoparticles: what we have learned so far? *J Nanopart Res* 12:2313–2333 (2010).
16. Chen YS, Hung YC, Liao I, Huang GS Assessment of the *in vivo* toxicity of gold nanoparticles. *Nanoscale Res Lett* 4:858–864(2009).
17. Cho EC, Xie JW, Wurm PA, Xia YN Understanding the role of surface charges in cellular adsorption versus internalization by selectively removing gold nanoparticles on the cell surface with a I2/KI etchant. *Nano Lett* 9:1080–1084 (2009a).
18. Franchini M.C., Ponti J., Lemor R, Fournelle M., Broggi F., Locatelli E. Polymeric entrapped thiol-coated goldnanorods: cytotoxicity and suitability as molecular optoacoustic contrast agent. *J. Mater. Chem.*, 2010, 20, 10908-10914. doi: 10.1039/C0JM02209H.
19. Qiu L., Larson T.A., Vitkin E., Guo L., Hanlon E.B., Itzkan I., Sokolov K.V., Perelman L.T. Gold nanorod light scattering labels for biomedical imaging. *Biomed Opt Express*. 2010, 1(1): 135–142.
20. Qu M, Mallidi S., Mehrmohammadi M., Truby R., Homan K., Joshi P., Chen Y-S, Konstantin Sokolov K., Emelianov S. Magneto-photoacoustic imaging *Biomed Opt Express*. 2011 2(2): 385–396.
21. Cho WS, Cho MJ, Jeong J, Choi M, Cho HY, Han BS, Kim HS, Kim HO, Lim YT, Chung BH Acute toxicity and pharmacokinetics of 13 nm-sized PEG-coated gold nanoparticles. *Toxicol Appl Pharmacol* 236:16–24 (2009b)
22. Kim C., Erpelding T.N., Jankovic L., Pashley M.D., Wang L.V. Deeply penetrating *in vivo* photoacoustic imaging using a clinical ultrasound array system. *Biomed Opt Express*. 2010 August 2; 1(1): 278–284.